Illusory bending of a rigidly moving line segment: Effects of image motion and smooth pursuit eye movements

Lore Thaler Department of Psychology, The Ohio State University, Columbus, OH, USA

James T. Todd Department of Psychology, The Ohio State University, Columbus, OH, USA

Miriam Spering Psychologisches Institut, Justus-Liebig-Universität, Gießen, Germany

Karl R. Gegenfurtner Psychologisches Institut, Justus-Liebig-Universität, Gießen, Germany

Four experiments in which observers judged the apparent "rubberiness" of a line segment undergoing different types of rigid motion are reported. The results reveal that observers perceive illusory bending when the motion involves certain combinations of translational and rotational components and that the illusion is maximized when these components are presented at a frequency of approximately 3 Hz with a relative phase angle of approximately 120°. Smooth pursuit eye movements can amplify or attenuate the illusion, which is consistent with other results reported in the literature that show effects of eye movements on perceived image motion. The illusion is unaffected by background motion that is in counterphase with the motion of the line segment but is significantly attenuated by background motion that is in-phase. This is consistent with the idea that human observers integrate motion signals within a local frame of reference, and it provides strong evidence that visual persistency cannot be the sole cause of the illusion as was suggested by J. R. Pomerantz (1983). An analysis of the motion patterns suggests that the illusory bending motion may be due to an inability of observers to accurately track the motions of features whose image displacements undergo rapid simultaneous changes in both space and time. A measure of these changes is presented, which is highly correlated with observers' numerical ratings of rubberiness.

Keywords: motion perception, motion integration, bending motion, nonrigid motion, rigid motion, smooth pursuit eye movements

Citation: Thaler, L., Todd, J. T., Spering, M., & Gegenfurtner, K. R. (2007). Illusory bending of a rigidly moving line segment: Effects of image motion and smooth pursuit eye movements. *Journal of Vision, 7*(6):9, 1–13, http://journalofvision.org/7/6/9/, doi:10.1167/7.6.9.

Introduction

Since the seminal work of Wallach (1935), it has long been recognized that the motions of smooth contours can be perceptually ambiguous. Consider, for example, the rotating ellipse that is presented in Auxiliary Movie 1. Although the ellipse is rotating rigidly in the image plane, it appears perceptually to be undergoing a nonrigid deformation (see Hildreth, 1984; Weiss & Adelson, 2000). The reason for this effect is that all points along the contour are visually indistinguishable so that it is not possible to measure the component of motion that is parallel to the contour at any given location. If, however, the pattern contains some distinct identifiable points, as in Auxiliary Movie 2, then the unambiguous motions of those features can constraint the interpretation of the contour motion, resulting in the perception of rigid rotation.

The experiments described in Wallach's (1935) original monograph all involved the translatory motions of straight-line contours. The perceptual ambiguity in that case is typically quite constrained. Although observers may perceive an illusory direction of motion, the moving contour always appears rigid. Indeed, this should not be surprising, given that the collinearity of the contour is never altered.

There is an interesting parlor demonstration called "the rubber pencil illusion" that is especially compelling because it violates this basic intuition. If a pencil is held loosely off center and wiggled up and down, it can appear to undergo a nonrigid bending motion (see Figure 1), although the pencil remains physically straight at all times. Note that this illusion occurs despite the presence of trackable features at the endpoints of the moving pencil and the absence of any contour curvature in its optical projection.

doi: 10.1167/7.6.9 Received August 24, 2006; published April 20, 2007 ISSN 1534-7362

Figure 1. A schematic illustration of the rubber pencil illusion.

The first scientific investigation of the rubber pencil illusion was performed by Pomerantz (1983). He presented observers with computer-generated displays of a rigid line segment undergoing various combinations of translation and rotation, and he asked them to rate the apparent "rubberiness" of each display on a 100-point scale. Figure 2 shows a static representation of four of the conditions used in that study. Each panel depicts a superposition of all of the discrete frames of a particular motion sequence. Figure 2A shows a horizontal line segment whose vertical position varies sinusoidally over time; Figure 2B shows a line segment whose orientation varies sinusoidally over time; and Figures 2C and 2D show different combinations of these basic translational and rotational components. Note in the latter two conditions how the motion trace produces a smoothly curved envelope. Pomerantz suggested that it is the curvature of the densest motion trace that leads to the illusory perception of bending, and he argued that this may be due to visual persistence at early levels of processing, perhaps even in the retina.

The research described in this article was designed to test several critical aspects of this hypothesis. Experiment 1 was similar to Pomerantz's original study in that it compared observers' rigidity ratings for moving line segments with varying combinations of translational and rotational components. Experiment 2 investigated the tuning properties of the illusion with respect to the relative phase angles and speeds of these components. In Experiment 3, observers' eye movements were manipulated to evaluate the separate effects of distal and retinal motion on the perception of illusory bending; finally, in Experiment 4, the motion of the background was manipulated to compare the effects of relative and absolute motion.

Experiment 1

Methods

Apparatus

The experiment was conducted using a Dell Dimension 8300 PC with an ATI Radeon 9700 PRO graphics card. Stimuli were presented on a 21-in. CRT (Mitsubishi Diamond Pro 97TXM) at a temporal resolution of 120 Hz and a spatial resolution of 800 (H) × 600 (V) pixels. The active display area subtended 38.7 × 29 cm, and the display was positioned at a distance of 35 cm from the observer. Displays were viewed binocularly in a darkened room, and a chin rest was used to restrain head movements.

Stimuli

Stimuli consisted of dotted black line segments (21 horizontally aligned, equally spaced dots) moving in front of a homogeneous, gray background (mean luminance, 39 cd/m^2). The length of these lines subtended 4.04° of visual angle, and each dot subtended 0.1° of visual angle. There were eight possible patterns of motion, generated by different combinations of translational and rotational oscillatory motion. The amplitude of the rotational component refers to the angle through which the line is rotated around its midpoint. It could be either 0° or 90°. The amplitude (total vertical excursion) of the translatory motion component could be 0°, 2.02°, or 4.04° of visual angle. When translational and rotational motions were combined, the relative phase angle between the two components was 125°. Examples of four different motion patterns are illustrated in Panels A–D of Figure 3. Each panel in this figure depicts a superposition of all of the discrete frames of a particular motion sequence. In the actual experiment, each 40-frame sequence was presented over time at a rate of 3 Hz. Half of the displays contained an additional 360° linear rotation at a constant angular velocity around the center of the moving line segment at a rate of 0.33 Hz to increase the complexity of the motion traces. Motion traces for the four displays with linear rotation are presented in Figures 3E–3H. The equations

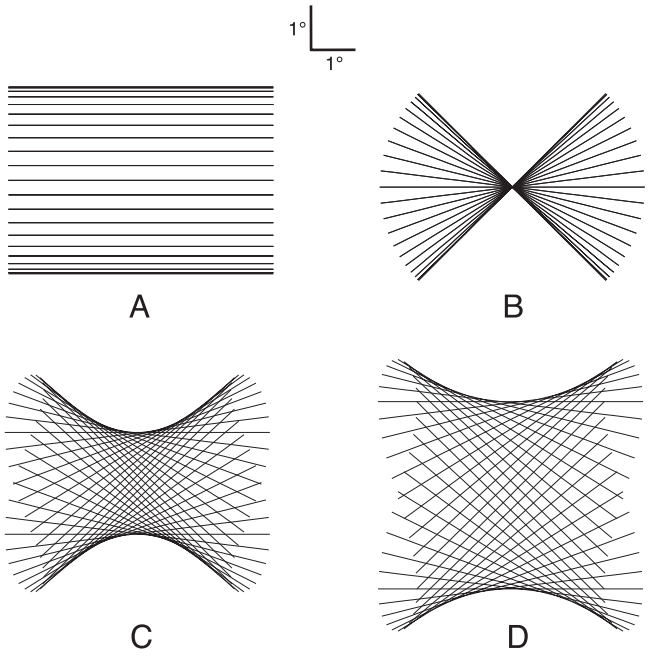

Figure 2. Static representations of four motion displays used by Pomerantz (1983). Each panel depicts a superposition of all of the discrete frames of a particular motion sequence.

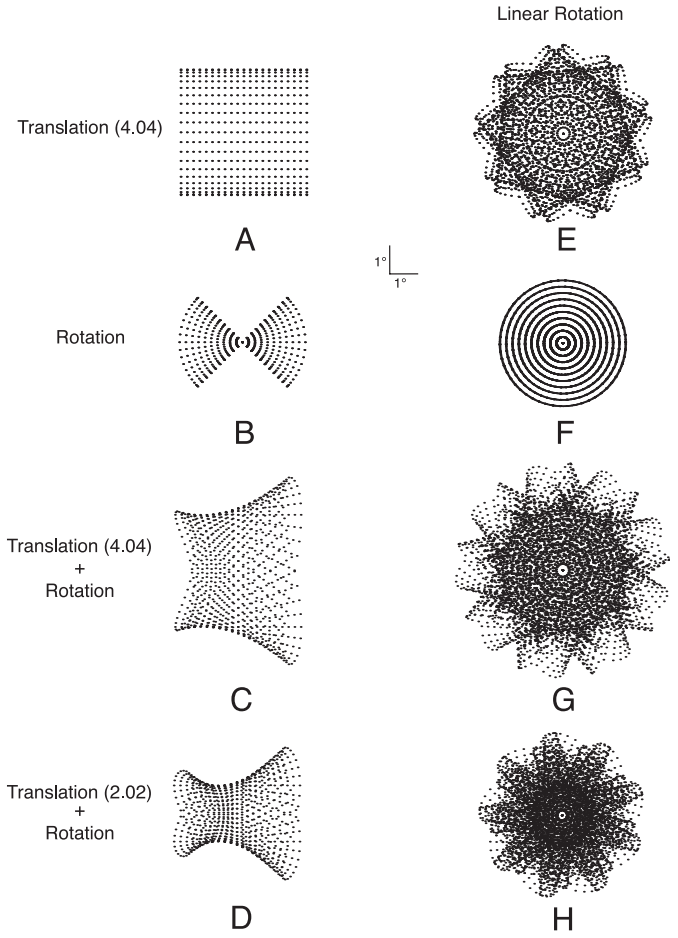

Figure 3. Static representations of the motion displays used in Experiment 1. Each panel on the left depicts a superposition of the 40 discrete frames of a particular motion sequence. Panels on the right show the motion pattern that was created by combining the pattern on the left with a linear rotation around the origin at a constant angular velocity over 360 discrete frames.

that describe the stimulus motion are shown in the Appendix.

Procedure

At the beginning of an experimental session, the rubber pencil illusion was demonstrated to the observer using an actual pencil. All observers spontaneously reported the percept of bending. The experimenter then read a standardized script in which the basic design of the experiment was described. On each trial, a motion display was presented on a computer monitor directly in front of the observer. A second monitor located off to the side displayed a numerical rating between 0 and 10 that could be adjusted by clicking the right and left buttons on a handheld computer mouse. Observers were instructed to rate the rubberiness of each motion pattern on this scale such that higher ratings indicated greater degrees of perceived rubberiness. A base rating of 0 was displayed at the beginning of each trial. When observers were satisfied with their setting, they proceeded to the next trial by hitting "enter" on the computer keyboard. It was possible to move backward in the sequence to revise settings, and many observers made use of this option to compare stimuli prior to rating them. Displays were presented in a random sequence for each observer. During debriefings, all observers reported that they felt confident in their settings and that various displays appeared nonrigid to them.

Observers

The displays were rated by eight observers, including one of the authors (J. T.) and seven others who were naïve to the purposes of the experiment. All observers had either normal or corrected-to-normal vision.

Results and discussion

Because observers were not required to use the full range of the rating scale, the results were normalized for each observer by dividing every rating by the maximum rating assigned by that observer. Figure 4 shows average normalized rubberiness rating across all observers for each of the different experimental conditions. Error bars denote standard errors of the mean within each group.

It is important to note when evaluating these results that Displays A–D are a near replication of those used by

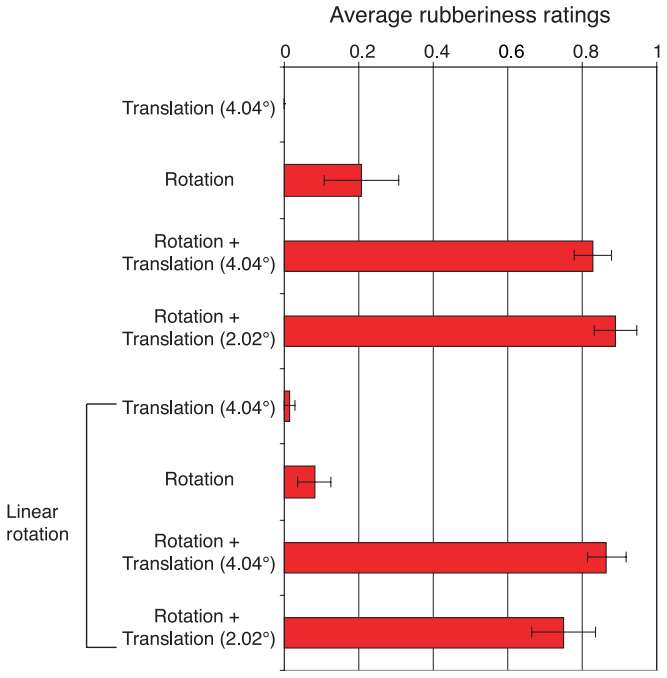

Figure 4. The average rubberiness ratings obtained in Experiment 2 for the different experimental conditions illustrated in Figure 3.

Pomerantz (1983), and they produced similar results. That is to say, the displays in which the densest motion trace is curved (C and D) were perceived as rubbery, whereas those in which the densest motion trace is straight (A and B) were perceived as relatively rigid. Conditions E–H were designed to test the generality of this finding. These displays were identical to those in Conditions A–D, except that they included an additional 360° rotational component at a constant angular velocity. Note in Figure 3 that this additional rotation caused the densest motion trace of all motion patterns to be curved, yet the results in Figure 4 show clearly that it had no significant effect on the observers' ratings. This finding suggests, therefore, that the apparent bending that occurs in the rubber pencil illusion cannot be explained based solely on the curvature of the densest motion trace.

The reliability of these results was confirmed using an analysis of variance. The observers' rubberiness ratings for the displays that contained a combination of translational and rotational oscillatory motion (C, D, G, and H) were significantly larger than the ratings obtained for the remaining displays (A, B, E, and F), $F(1, 7) = 337.02$, $p < .001$, and this one comparison accounted for 96% of the between-display variance. No other comparisons among the different conditions were statistically significant.

Experiment 2

Experiment 2 was designed to determine which presentation speeds and relative phase angles between the rotational and translational motion components are optimal for the perception of bending motion in our displays. Observers were asked to adjust the speed and relative phase angle between the two components to maximize the perception of bending.

Methods

Stimuli

Stimuli consisted of dotted black line segments (21 horizontally aligned, equally spaced dots) moving in front of a homogeneous, gray background (mean luminance, 39 cd/m^2). Observers saw motion displays in two different experimental conditions. In the "speed" condition, the translational and rotational motion was presented with nine different relative phase angles (0°, 22.5°, 45°, 67.5°, 90°, 112.5°, 135°, 157.5°, and 180°). For a given phase angle, observers could vary the speed of the motion such that the overall pattern of oscillation could occur at 1.5, 2, 2.5, 3, or 3.75 Hz. Similarly, in the "phase" condition, the motion pattern was presented at five different speeds (1.5, 2, 2.5, 3, or 3.75 Hz), and for any given speed, observers could adjust the relative phase angle of the translational and rotational components with possible values of 0°, 22.5°, 45°, 67.5°, 90°, 112.5°, 135°, 157.5°, and 180°.

Procedure

The speed and phase conditions were presented in separate blocks. In the speed condition, observers were instructed to adjust the speed of the motion pattern to maximize the apparent bending. On each trial, observers saw a motion display on a computer monitor and they adjusted the speed by pressing the "up" and "down" keys on a computer keyboard. After adjusting the optimal speed for all motion patterns, observers were instructed

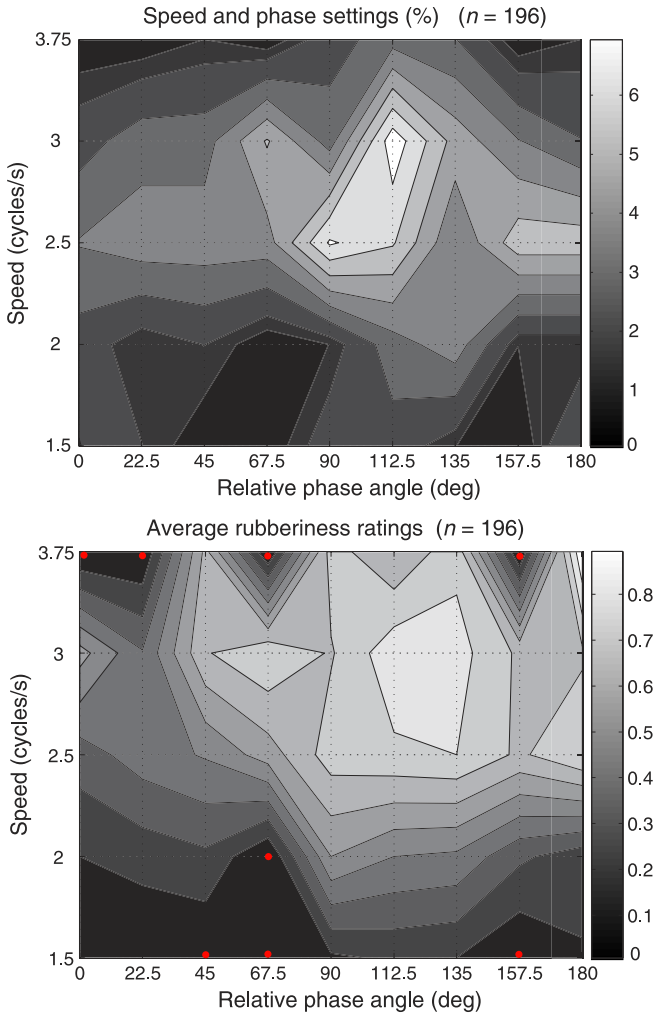

Figure 5. Results from Experiment 2. The top panel shows the relative frequency of maximum rubberiness ratings for each combination of speed (represented on the vertical axis) and relative phase (represented on the horizontal axis). Black image regions indicate relative frequencies of zero. The bottom panel shows average rubberiness ratings for the various motion conditions. Red circles indicate that a condition had not been selected (and therefore not rated) by any observer.

to go back through the stimulus sequence and to rate each motion pattern they had created with respect to its apparent bending on a rating scale of 0 to 10, as in Experiment 1. Each of the nine relative phase angles was presented twice in random order. In one presentation, stimulus motion was initiated with a speed of 3.75 Hz, and in the other, it was initiated with a speed of 1.5 Hz. The procedure was identical in the phase condition except that the observers adjusted the relative phase of the translational and rotational components rather than their speeds.

Observers

The displays were evaluated by eight observers, including two of the authors (L. T. and J. T.) and five others who were naïve to the purposes of the experiment. All observers had either normal or corrected-to-normal vision.

Results and discussion

The contour plot presented in the top panel of Figure 5 shows the frequency of maximum rubberiness settings for

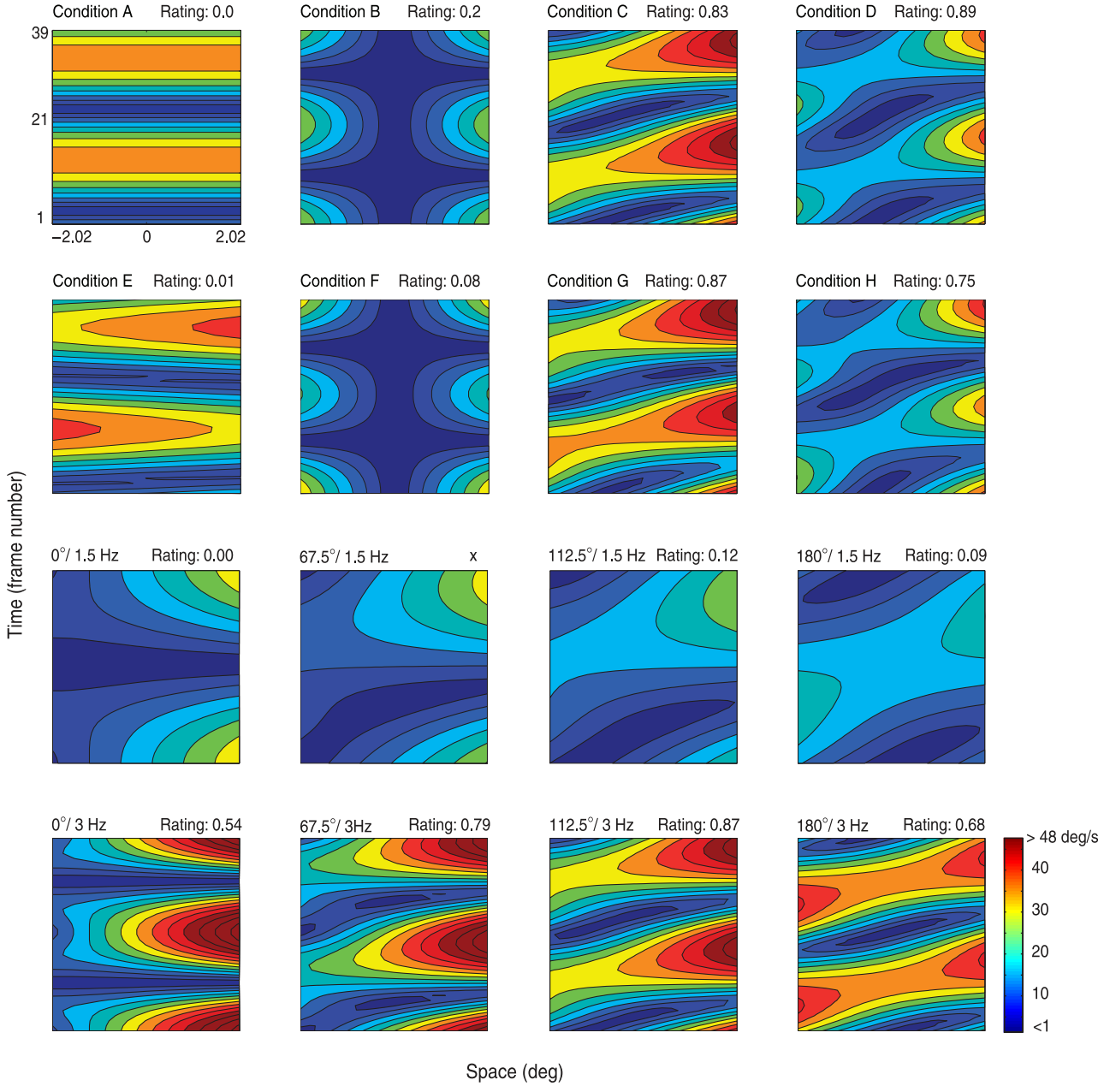

Figure 6. Contour plots of displacements for selected motion patterns from Experiments 1 and 2 at each position along the line segment (indicated on the horizontal axis) at each moment in time (indicated on the vertical axis). The text above each panel specifies the experimental condition and average judged rubberiness. Crosses indicate that a condition was not selected (and therefore not rated) by any observer.

all possible combinations of speed and relative phase that were obtained in both experimental conditions. The bottom panel of Figure 5 shows the average rubberiness ratings for the motion patterns generated from these settings. Red circles indicate that a condition had not been selected (% = 0) and, therefore, not rated by any observer. Note in both cases that there is a tuning curve along both dimensions, such that the rubberiness is maximized for speeds of 2.5 and 3 Hz, and relative phase angles of approximately 120°. An interesting finding was that the adjustment task produced sharper tuning functions than the rating task. This might be due to the fact that the adjustment task involves a direct ordinal comparison between displays with different parameter settings, which might make it a more sensitive measure in this context.

It is useful to consider how the displacement of each visible point varied over space and time to better understand why some conditions may appear more rubbery than others. The contour plots presented in Figure 6 show the displacements $d = f(p, t)$ at each position (p) along a moving line at each moment in time (t) for selected conditions from Experiments 1 and 2. The text above each plot shows experimental condition and average judged rubberiness for that condition. It is interesting to note when evaluating these plots that the appearance of rubberiness was larger for displays in which the displacements at each point varied simultaneously in both space and time. These can be identified in Figure 6 by the preponderance of diagonally oriented contours.

To provide a more precise quantitative measure of this observation, we computed the displacement gradients

$$G_d = \left(\frac{\partial d}{\partial p}, \frac{\partial d}{\partial t}\right) \quad (1)$$

for a large sample of points within each contour plot (n = 780) and multiplied the spatial and temporal components of the gradient at each point. The absolute values of the products obtained over an entire sample were then averaged together to provide an overall measure (C) of the extent to which the displacement in each display varied simultaneously in both space and time:

$$C = \frac{1}{n}\sum_{i=1}^{n}\left|\frac{\partial d_i}{\partial p}\frac{\partial d_i}{\partial t}\right|. \quad (2)$$

Figure 7 shows the average rubberiness rating in each condition as a function of the average space–time gradient product measure. The solid curve in this figure is the best fitting sigmoid function, which accounts for 77% of the variance in observers' judgments among the different display conditions. Note that the rubberiness ratings increase linearly over small to moderate values of C and then reach an asymptote as the gradients become larger. These findings suggest that the illusory bending motion may be due to an inability of observers to accurately track the motions of features whose image displacements undergo rapid simultaneous changes in both space and time.

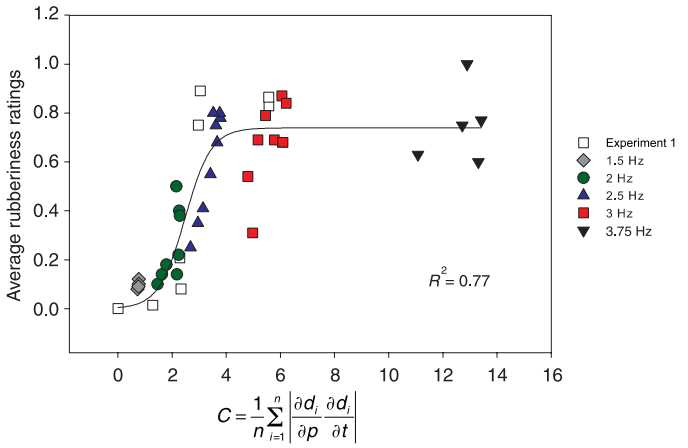

Figure 7. Observers' average rubberiness ratings from Experiments 1 and 2 plotted against the average space–time gradient product. The solid line depicts the best fitting sigmoid function $f(x) = 0.74/(1 + e^{-(x - 2.5)/0.5)})$.

Experiment 3

Motion signals on the retina typically arise from a mixture of the motions of external objects (i.e., distal motion) and movements of the observer's eye and head relative to the external environment. In everyday situations, however, humans usually perceive a scene within an external frame of reference, thus indicating that they are able to successfully discount the movements of their eyes and head. Note that this provides a potentially useful test of Pomerantz's (1983) hypothesis that the rubber pencil illusion arises from motion blur on the retina. If that is the case, if observers track the translatory component of a moving line segment with smooth pursuit eye movements, then the retinal motion will be reduced to pure rotation, and the display should be perceived as rigid. Experiment 3 was designed to test this prediction.

Methods

Apparatus

Stimuli were displayed on a 21-in. CRT monitor (ELO Touchsystems, Fremont, CA, USA) by an ASUS V8170 (GeForce 4MX 440) graphics board at a temporal resolution of 100 Hz noninterlaced and a spatial resolution

of 1,024 (H) × 768 (V) pixels. The active display area subtended 39 × 29.3 cm, and the display was positioned at a distance of 47 cm from the observer.

Eye-movement recording

Eye position signals were recorded with a head-mounted, video-based eye tracker (EyeLink II; SR Research Ltd., Osgoode, Ontario, Canada) and were sampled at 250 Hz. The apparatus was calibrated at the beginning of the main experiment by instructing the observer to fixate single dots that appeared successively at nine different positions on the monitor. Based on the results of this calibration, the better eye was chosen automatically by the system, and eye position was recorded from this eye. Observers were seated with their heads stabilized with a chin rest. They viewed the display binocularly through natural pupils. A PC controlled stimulus display and data collection.

Stimuli

Each stimulus contained a smooth black line segment moving in front of a homogeneous, gray background (mean luminance 39 cd/m^2). The length of this line was 4.04° and its width was 0.1°. All of the displays included a rotary oscillation, in which the line segment rotated back and forth through an angle of 90° at a rate of 2.5 Hz. On half the trials, this rotary oscillation was the only source of distal motion. On the remaining trials, an additional component of motion was added, in which the center of the line segment was translated along an elliptical orbit around the center of the display screen at a rate of 0.83 Hz. The horizontal and vertical axes of the elliptical trajectory subtended 8.08° and 4.84°, respectively. Both of these distal motion conditions were observed with the eyes fixated on a stationary point and with the eyes tracking a moving fixation point along an 8.08° × 4.84° elliptical trajectory. These different combinations of distal and eye motion resulted in four basic experimental conditions that are illustrated in Figure 8. The equations used to generate these motions are given in the Appendix.

Procedure

Each trial began with a stationary visual target whose diameter subtended 0.5° of visual angle, and the color of this target indicated whether the upcoming motion display would include a stationary (blue) or moving (red) visual target. Observers initiated a trial by pressing an assigned button. The EyeLink II system then performed a drift correction to correct for shifts of the head-mounted tracking system. Once this was achieved, the stimulus presentation was initiated after a random time interval between 200 and 400 ms. On trials that required smooth pursuit eye movements, the fixation point began to move as soon as the line segment appeared. After 2.4 s, the display motion was terminated, and observers rated its rubberiness on a rating scale from 0 to 4 by pressing assigned keys on the keyboard. Stimuli were presented in blocks of 20 trials containing five repetitions of the four experimental conditions. An experimental session included six blocks, the first of which was discarded as practice.

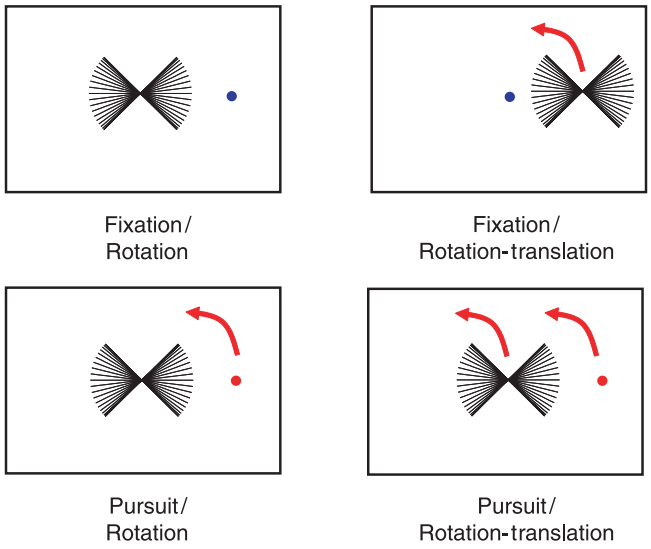

Figure 8. Illustrations of motion displays used in Experiment 3. The rotational motion of the line segment is represented by superimposing the 40 discrete frames of a rotational motion sequence. Translational, elliptical motion of the line segment or/and the eye is indicated by arrows. Dots illustrate the visual target in fixation (blue-colored target) or pursuit (red-colored target) conditions.

Observers

Ten observers participated in the experiment, including one of the authors (M. S.) and nine naïve observers who were selected from the observer pool at the University of Giessen, Germany, where the experiment was conducted. Observers were contacted via telephone and were paid for their participation. All observers had normal or corrected-to-normal vision and were highly trained in smooth pursuit tasks.

Analysis of eye movements

To compare perception of rubberiness in the different pursuit and fixation conditions, we had to ensure that observers had followed our instructions concerning eye movements and, furthermore, that eye movements were comparable in the pursuit and fixation conditions. Eye movements were analyzed in two steps. The first step was designed to remove any saccades from the overall position traces as described by Spering, Kerzel, Braun, Hawken, and Gegenfurtner (2005). Any movements that exceeded

15°/s in the fixation conditions or 45°/s in the pursuit conditions were considered as saccades and excluded from subsequent analyses. The remaining position traces were then smoothed, and the average eye velocity was divided by the average target velocity (17.19°/s) to determine the perceptual gain for each trial. If the resulting gain was above 0.23 for the fixation conditions or below 0.77 for the pursuit conditions, the trial was considered invalid. Trials were also considered invalid if observers blinked during the 2.4-s stimulus presentation.

Based on these criteria, one observer was excluded from further analysis because low pursuit gain resulted in too few valid trials in pursuit conditions ($n < 5$). Across the remaining nine observers, 10.4% of all trials ($n = 94$) were excluded from further analyses, all of them pursuit trials. Average eye-movement gain in the two pursuit conditions was 0.89 and 0.90, respectively (between-observer SD = 0.07 and 0.06, respectively). Average eye-movement gain in both fixation conditions was 0.09 (between-observer SD = 0.02 in both conditions). Only numerical ratings obtained in valid trials were considered for further analysis.

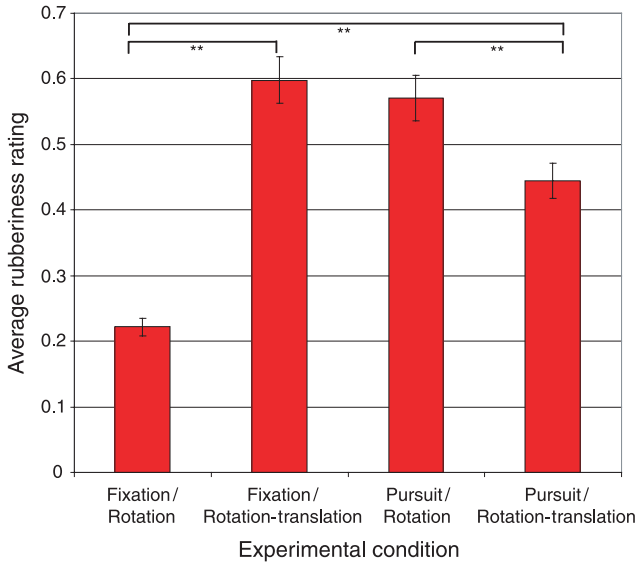

Figure 9. The average rubberiness ratings obtained in Experiment 3. **$p < .01$.

Results

The normalized ratings for each condition averaged over observers are presented in Figure 9. Error bars indicate standard error of the mean within each group. An analysis of variance revealed that there were significant main effects of distal motion, $F(1, 8) = 10.07$, $p < .05$, and eye motion, $F(1, 8) = 11.78$, $p < .01$, and a significant interaction, $F(1, 8) = 24.84$, $p < .001$. Additional post hoc paired-sample t tests (two sided) were performed to compare individual pairs of conditions. Significance is indicated in Figure 9 by asterisks.

If the apparent rubberiness of the displays were based entirely on the distal motion patterns, then there should be no significant differences between the fixation and pursuit conditions. If, on the other hand, the apparent rubberiness of the displays were based entirely on the retinal motion patterns, then the fixation/rotation and pursuit/rotation–translation conditions should both produce low rubberiness ratings, and the pursuit/rotation and fixation/rotation–translation conditions should both produce high rubberiness ratings. It is clear from Figure 9 that neither of these hypotheses can provide a complete account of the data, although retinal motion seems to be the predominant factor that influenced observers' judgments. Note, for example, that the pursuit/rotation and fixation/rotation–translation conditions both produced high rubberiness ratings, as would be expected based on a pure retinal motion hypothesis. This finding suggests that when a smooth pursuit eye movement is independent of a distal object's motion, then the eye movement is not discounted in the perceptual analysis of that motion (see also Brenner & van den Berg, 1994). However, when the eye movements tracked the motion of a distal object in the pursuit/rotation–translation condition, the results indicate that they were partially discounted. That is to say, the apparent rubberiness of the pursuit/rotation–translation displays was halfway between what would be expected from a pure retinal motion hypothesis and a pure distal motion hypothesis. Taken together, the results suggest that extra retinal signals are ignored when the eyes move on a different trajectory as the target but that they are partially accounted for when the line segment and the eye follow the same elliptical trajectory (see also Brenner & van den Berg, 1994).

It is important to note that pursuit gain was comparable in the two pursuit conditions. Thus, the data provide strong evidence that similar pursuit trajectories have different effects on the perception of bending motion, depending upon the direction of the pursuit trajectory with respect to the target trajectory. It could be argued that the retinal motion patterns in the pursuit and fixation conditions were not entirely equivalent because the pursuit conditions produced retinal motion at the edges of the monitor whereas the fixation conditions did not. However, it is not obvious how this would explain the differential effects of pursuit in the two distal motion conditions.

It is also interesting to note that the results of the present experiment have been replicated using dotted line segments. This replication was conducted at the Ohio State University on the apparatus described in Experiment 1 with the same participants as in Experiment 1. Although observers were instructed to pursue or fixate in the appropriate conditions, we did not confirm through eye-movement recordings the extent to which they complied with those instructions. Nevertheless, the results obtained

were comparable to those reported here. Similarly, we obtained equivalent results using an alternative analysis to evaluate eye movements that assessed fixation stability using a position criterion, instead of a gain criterion.

Experiment 4

One of the basic discoveries of Gestalt psychology is that the perceived trajectory of a moving object is not always determined by its relative motion with respect to the retina or the ground but may instead be based on its motion relative to other moving objects. The perceived motion of a rolling wheel provides an excellent example (see Duncker, 1929; Johansson, 1950; Rubin, 1927, for more examples). The trajectory of a single point on the wheel has the form of a cycloid, but its perceived trajectory is a simple rotary motion about the center of the wheel. Indeed, it is not possible to perceive the cycloidal trajectory, even if one tries, unless the point is presented in isolation. The question arises if the presence of an alternative frame of reference with respect to a moving background could influence the strength of the rubber pencil illusion. If so, it would provide another source of evidence that motion blur on the retina cannot be the sole cause of the illusion.

Methods

Apparatus

The display apparatus and eye tracker were identical to those used in Experiment 3. The apparatus was calibrated both at the beginning of the main experiment and after the first two experimental blocks.

Stimuli

The stimuli were divided into three different categories. Two standard control conditions were comparable to those used in the previous studies. In the rigid standard condition, a horizontal smooth black line segment translated up and down at a rate of 2.5 Hz against a homogeneous, gray background. In the bending standard condition, this translational component was combined with a 90° rotational motion with a relative phase angle of 125°. In the second category of displays, the line segments with both translational and rotational components were presented against a background of small randomly positioned squares. This background could be stationary, moving in-phase with the line segment or moving in counterphase with the line segment. Finally, in the third category of displays, the line segments with both translational and rotational components were presented within a larger rectangular figure that could move in-phase with the line segments or in counterphase. A schematic diagram of the seven different conditions is presented in Figure 10.

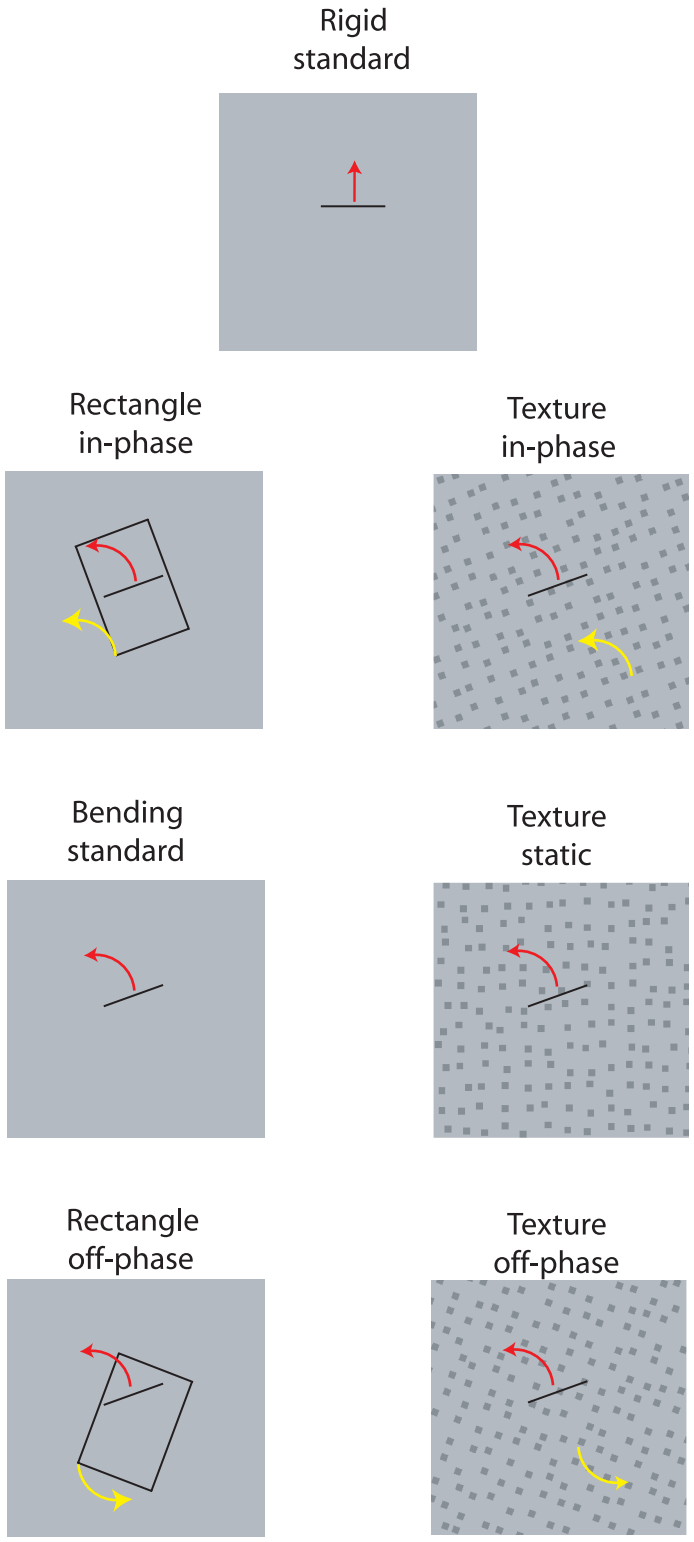

Figure 10. Illustrations of motion displays used in Experiment 4. Yellow arrows indicate background motion. Red arrows indicate motion of the line segment.

Procedure

Each trial began with a fixation target subtending 0.5° of visual angle that was located 2.6° above the center of the display. Observers initiated a trial by pressing an assigned button. The EyeLink II system then performed a drift correction to correct for shifts of the head-mounted tracking system. Once this was achieved, the stimulus presentation was initiated after a random time interval between 200 and 400 ms. Each trial included two different motion displays in successive 2-s intervals with a 0.5-s separation period. Observers were instructed to remain fixated on the target during the entire display period. Once the display was terminated, observers were required to judge which interval appeared more "rubbery" by pressing an appropriate key on the computer keyboard. They were instructed to judge only the motion of the central line segment and to ignore the background. Stimuli were presented in blocks of 42 trials containing seven repetitions of the seven experimental conditions. An experimental session included four blocks, the first of which was discarded as practice.

Observers

Ten observers with normal or corrected-to-normal vision participated in the experiment. All participants were experienced psychophysical observers and were selected from an observer pool at the University of Giessen, Germany. Observers were contacted via telephone and were paid for their participation.

Analysis of eye movements

To compare perception of rubberiness in the different conditions, we had to ensure that observers had fixated properly during the 4.5-s stimulus presentation. The analysis of eye movements differed from the one described for Experiment 3 in that we calculated the average eye velocity in degrees per second as a measure of fixation stability instead of relative gain. Eye velocity during both 2-s intervals was required to be less than 3°/s to be considered valid fixation. Otherwise, the trial was excluded from further analysis. Trials were also excluded from further analysis if the observer blinked during the 4.5-s stimulus presentation. Based on these criteria, 14.76% (n = 186) of all trials were excluded from further analyses across observers. Eye velocity was comparable across observers and experimental conditions for the remaining trials (average eye velocity = 1.83°/s, median = 1.85°/s, SD = 0.22°/s, range = 0.81°/s). As in Experiment 3, we also used an alternative analysis of eye movements that relied on a position criterion to assess fixation stability, with equivalent results.

Results

Table 1 shows the pattern of results combined over all observers for all of the possible pairwise comparisons among the different conditions. Values in each cell show the probability that the condition labeled in the column was rated as more rubbery than the condition labeled in the row. Values in parentheses indicate the number of trials over which each probability was computed.

To provide a summary of the data that takes into account possible differences between observers, we calculated for each observer and each condition the probability of that condition to be judged more bending over all its pairwise comparisons. Figure 11 shows the probability of each condition to be judged more rubbery over all of its possible pairwise comparisons averaged across observers. Error bars denote standard errors of the mean within each group, and asterisks indicate significant differences between conditions assessed via paired-sample t test (two sided). Note in the figure that when the background moves in counterphase with the moving line segment, it has no discernable effect on apparent rubberiness relative to the bending standard condition with a homogeneous background. However, if the line segment is presented against a static textured background or if the background motion is identical to that of the line segment, then the perception of rubberiness is intermediate between

	Rigid standard	Rectangle in-phase	Texture in-phase	Texture static	Bending standard	Texture off-phase	Rectangle off-phase
Rigid standard	X	.86 (50)	.98 (51)	.96 (48)	.96 (45)	.98 (50)	.98 (46)
Rectangle in-phase		X	.82 (50)	.72 (58)	.84 (49)	.85 (54)	.93 (54)
Texture in-phase			X	.55 (53)	.70 (53)	.73 (51)	.68 (53)
Texture static				X	.59 (56)	.57 (51)	.63 (51)
Bending standard					X	.45 (49)	.49 (47)
Texture off-phase						X	.51 (55)
Rectangle off-phase							X

Table 1. Results from Experiment 4. Each cell represents the probability of the condition denoted in the column to be judged more rubbery than the condition denoted in the row. Values in parentheses represent the number of pairwise comparisons used to compute probabilities in each cell.

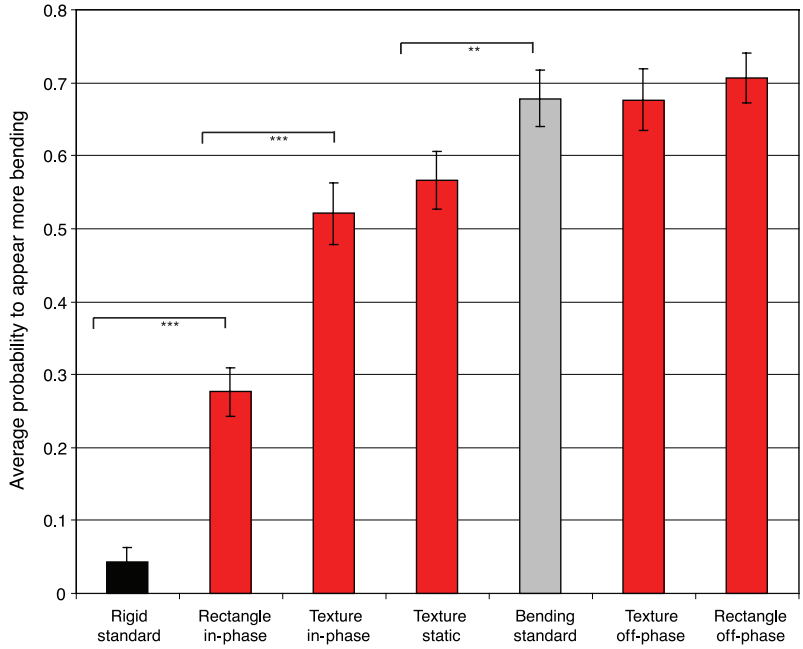

Figure 11. Results of Experiment 4. Bars represent the probability of a motion condition to appear more bending over all pairwise comparisons. Error bars indicate standard error of the mean within each group. $^{**}p < .01$, $^{***}p < .001$.

the rigid standard and bending standard conditions. These results are, in many ways, similar to those obtained with pursuit eye movements in Experiment 3. Both studies suggest that retinal motion is the predominant factor for determining the strength of the rubber pencil illusion but that the effect can be attenuated if the motion of the pencil is the same as its local frame of reference—either the eye or the background.

Discussion

The research described in the present article was designed to investigate an intriguing phenomenon called "the rubber pencil illusion." If a pencil is held loosely off center and wiggled up and down, it can appear to undergo a nonrigid bending motion (see Figure 1), although the pencil remains physically straight at all times. This phenomenon was investigated previously by Pomerantz (1983), who suggested that the apparent rubberiness is caused by curvature of the densest motion trace on the retina arising from motion blur. Experiment 1 of the present series replicated Pomerantz's findings with comparable displays, but it also included additional conditions with curved motion traces that were nonetheless perceived as rigid. This finding provides strong evidence that some other factor must also play a role in producing the apparent nonrigidity in the rubber pencil illusion.

Experiment 2 was designed to explore the relative sensitivity of this phenomenon to variations in speed of a moving line segment and the relative phase angle between its translational and rotational components. The results reveal that variations in these parameters can have a large effect on how a moving line segment is perceived. The appearance of rubberiness is maximized for speeds of 2.5 and 3 Hz and relative phase angles of approximately 120°, and it drops off sharply when the parameters deviate from these optimal values.

Experiments 3 and 4 were designed to investigate whether the illusory rubberiness can be influenced by relative frames of reference other than the retina. The results reveal that if a line segment's translational motion is quite different from that of the eye (Experiment 3) or the background (Experiment 4), then the appearance of rubberiness is reliably predicted by its relative motion with respect to the retina. If, on the other hand, the line segment's motion is appropriately yoked to the motions of the eye or the background, then the appearance of rubberiness can be significantly attenuated, although not eliminated entirely. These findings suggest that the illusion is primarily determined by motion relative to the retina but that other frames of reference may also have an influence under appropriate circumstances.

It is important to keep in mind when evaluating these results that the patterns of motion in all of our displays were computationally unambiguous because each individual dot in Experiments 1 and 2 provided a trackable feature, as did the endpoints of the moving line segments in Experiments 3 and 4 (see Reichardt, Egelhaaf, & Schlögl, 1988; Uras, Girosi, Verri, & Torre, 1988). Nevertheless, although the actual motion of each display was perfectly rigid, observers often perceived the line

segments as undergoing a nonrigid bending transformation. An analysis of the motion patterns in Experiments 1 and 2 suggests that this illusory bending motion may be due to an inability of observers to accurately track the motions of features whose image displacements undergo rapid simultaneous changes in both space and time. The extent of these changes can be measured quite simply by multiplying the speed gradients in both space and time, and this measure can account for 77% of the variance in the observers' rubberiness ratings among the different display conditions.

Although the space–time gradient product measure can reliably predict the apparent rubberiness of these displays, it remains to be determined how this finding might be incorporated into existing models of flow field estimation (e.g., Hildreth, 1984; Reichardt et al., 1988; Uras et al., 1988, Weiss, 1997, 1998; Yuille & Grzywacz, 1988). There are two critical aspects of these results that remain to be addressed by future research. One is to explain why the motions of trackable features in these displays do not provide sufficient information to perceptually determine the correct pattern of motion. Moreover, even if one interpreted the dotted line segments as if they were continuous contours, it is not immediately obvious based on existing theory why these line segments should appear to bend. One popular explanation for previous demonstrations of illusory nonrigid motions of continuous contours (e.g., see Auxiliary Movie 1) is that observers are biased to select an interpretation that is maximally smooth (Hildreth, 1984; Horn & Schunck, 1981; Weiss, 1997, 1998; Yuille & Grzywacz, 1988). However, the maximally smooth interpretation of a moving straight line is always a rigid motion. Thus, an adequate explanation of the rubber pencil illusion is likely to require some other type of constraint.

Appendix A

The stimulus motion used in the current experiments is described below as the spatial position (x, y) of a point as a function of time t, measured as an integer number of frames after $t = 0$. The sinusoidal rotational and translational motion components of this motion are

$$\mathrm{rot}(t) = A_\theta \sin(\omega_s t) \tag{A1}$$

$$\mathrm{trans}(t) = A_\tau \sin(\omega_s t + \varphi), \tag{A2}$$

where A_θ is the angular amplitude (in radians) through which a given point is rotated around the origin of the coordinate system, A_τ is the amplitude of the translational motion component (in degrees of visual angle) relative to the origin, φ is the relative phase angle (in radians) between rotational and translational modulation, and $\omega_s = \pi/20$ in the current experiments. The x and y spatial coordinates of any point as a function of time, then, are sums of rotational and translational components:

$$x(t) = x\cos(\mathrm{rot}(t)) + y\sin(\mathrm{rot}(t)) \tag{A3}$$

$$y(t) = -x\sin(\mathrm{rot}(t)) + y\cos(\mathrm{rot}(t)) + \mathrm{trans}(t). \tag{A4}$$

The x and y spatial coordinates of any point after a linear rotation is applied to each of the sinusoidal motion patterns, as it was done in Experiment 1, are

$$x(t, \mathrm{lin}) = x(t)\cos(\omega_{\mathrm{lin}} t) + y(t)\sin(\omega_{\mathrm{lin}} t) \tag{A5}$$

$$y(t, \mathrm{lin}) = -x(t)\sin(\omega_{\mathrm{lin}} t) + y(t)\cos(\omega_{\mathrm{lin}} t), \tag{A6}$$

where $\omega_{\mathrm{lin}} = \pi/180$ in the current experiments.

The x and y spatial coordinates of any point after an elliptical translation is applied to the sinusoidal rotation, as it was done in Experiment 3, are

$$x(t, \mathrm{ell}) = x\cos(\mathrm{rot}(t)) + y\sin(\mathrm{rot}(t)) + a\cos(\omega_{\mathrm{ell}} t) \tag{A7}$$

$$y(t, \mathrm{ell}) = -x\sin(\mathrm{rot}(t)) + y\cos(\mathrm{rot}(t)) + b\sin(\omega_{\mathrm{ell}} t), \tag{A8}$$

where $\omega_{\mathrm{ell}} = \pi/60$, $a = 4.04°$, and $b = 2.42°$ in the current experiments.

The x and y spatial coordinates of any point as a function of time t that is moving off-phase with the line segment, as it was done in Experiment 4, are

$$x(t, \mathrm{off}) = x\cos(-\mathrm{rot}(t)) + y\sin(-\mathrm{rot}(t)) \tag{A9}$$

$$y(t, \mathrm{off}) = -x\sin(-\mathrm{rot}(t)) + y\cos(-\mathrm{rot}(t)) - \mathrm{trans}(t). \tag{A10}$$

Acknowledgments

The authors thank Stephan Ripke for his help with the data collection at the University of Giessen, Germany, and Delwin Lindsey, Martin Nikolov, and Doris Braun for many helpful and insightful discussions. The authors thank Delwin Lindsey for helpful comments on a previous version of the manuscript.

Commercial relationships: none.
Corresponding author: Lore Thaler.
Email: thaler.11@osu.edu.
Address: Department of Psychology, The Ohio State University, 1827 Neil Avenue, Columbus, OH 43210, USA.

References

Brenner, E., & van den Berg, A. V. (1994). Judging object velocity during smooth pursuit eye movements. *Experimental Brain Research, 99,* 316–324. [PubMed]

Duncker, K. (1929). Über induzierte Bewegung. Ein Beitrag zur Theorie optisch wahrgenommener Bewegung. [On induced motion. A contribution to the theory of visually perceived motion]. *Psychologische Forschung, 12,* 180–259.

Hildreth, E. C. (1984). *The measurement of visual motion.* Cambridge, MA: MIT Press.

Horn, B. K. P., & Schunck, B. G. (1981). Determining optical flow. *Artificial Intelligence, 17,* 185–203.

Johansson, G. (1950). *Configurations in event perception.* Uppsala: Almquist & Wiksell.

Pomerantz, J. R. (1983). The rubber pencil illusion. *Perception and Psychophysics, 33,* 365–368. [PubMed]

Reichardt, W., Egelhaaf, M., & Schlögl, R. W. (1988). Movement detectors provide sufficient information for local computation of 2-D velocity field. *Naturwissenschaften, 75,* 313–315. [PubMed]

Rubin, E. (1927). Visuell wahrgenommene wirkliche Bewegungen [Visually perceived genuine motions]. *Zeitschrift für Psychologie, 103,* 384–392.

Spering, M., Kerzel, D., Braun, D. I., Hawken, M. J., & Gegenfurtner, K. R. (2005). Effects of contrast on smooth pursuit eye movements. *Journal of Vision, 5* (5):6, 455–465, http://journalofvision.org/5/5/6/, doi:10.1167/5.5.6. [PubMed] [Article]

Uras, S., Girosi, F., Verri, A., & Torre, V. (1988). A computational approach to motion perception. *Biological Cybernetics, 60,* 79–87.

Wallach, H. (1935). Ueber visuell wahrgenommene Bewegungsrichtung [On visually perceived direction of motion]. *Psychologische Forschung, 20,* 325–380.

Weiss, Y. (1997). Smoothness in layers: Motion segmentation using nonparametric mixture estimation. In *Proceedings of the 1997 IEEE Computer Society Conference on Computer Vision and Pattern Recognition* (pp. 520–526). Los Alamitos, CA: IEEE.

Weiss, Y. (1998). *Bayesian motion estimation and segmentation.* Unpublished doctoral dissertation, Department of Brain and Cognitive Science, Massachusetts Institute of Technology, Cambridge, MA.

Weiss, Y., & Adelson, E. H. (2000). Adventures with gelatinous ellipses: Constraints on models of human motion analysis. *Perception, 29,* 543–566. [PubMed]

Yuille, A. L., & Grzywacz, N. M. (1988). A computational theory for the perception of coherent visual motion. *Nature, 333,* 71–74. [PubMed]